

***FAT1*, a direct transcriptional target of E2F1, suppresses cell proliferation, migration and invasion in esophageal squamous cell carcinoma**

Yu Wang¹, Guangchao Wang², Yunping Ma¹, Jinglei Teng¹, Yan Wang³, Yongping Cui⁴, Yan Dong⁵, Shujuan Shao⁶, Qimin Zhan^{1,3}, Xuefeng Liu¹

¹Institute of Cancer Stem Cell, Dalian Medical University, Dalian 116044, China; ²State Key Laboratory of Molecular Oncology, National Cancer Center/National Clinical Research Center for Cancer/Cancer Hospital, Chinese Academy of Medical Sciences and Peking Union Medical College, Beijing 100021, China; ³Key Laboratory of Carcinogenesis and Translational Research (Ministry of Education/Beijing), Laboratory of Molecular Oncology, Peking University Cancer Hospital & Institute, Beijing 100142, China; ⁴Shenzhen Peking University-The Hong Kong University of Science and Technology (PKU-HKUST) Medical Center, Peking University Shenzhen Hospital, Shenzhen 518036, China; ⁵College of Stomatology, Dalian Medical University, Dalian 116044, China; ⁶Key Laboratory of Proteomics, Dalian Medical University, Dalian 116044, China
Correspondence to: Xuefeng Liu. Institute of Cancer Stem Cell, Dalian Medical University, Dalian 116044, China. Email: ixuee@sina.com; Qimin Zhan. Institute of Cancer Stem Cell, Dalian Medical University, Dalian 116044, China; Key Laboratory of Carcinogenesis and Translational Research (Ministry of Education/Beijing), Laboratory of Molecular Oncology, Peking University Cancer Hospital & Institute, Beijing 100142, China. Email: zhanqimin@bjmu.edu.cn.

Abstract

Objective: Growing evidence indicates that FAT atypical cadherin 1 (*FAT1*) has aberrant genetic alterations and exhibits potential tumor suppressive function in esophageal squamous cell carcinoma (ESCC). However, the role of *FAT1* in ESCC tumorigenesis remains not well elucidated. The aim of this study was to further investigate genetic alterations and biological functions of *FAT1*, as well as to explore its transcriptional regulation and downstream targets in ESCC.

Methods: The mutations of *FAT1* in ESCC were achieved by analyzing a combined study from seven published genomic data, while the copy number variants of *FAT1* were obtained from an analysis of our previous data as well as of The Cancer Genome Atlas (TCGA) and Cancer Cell Line Encyclopedia (CCLE) databases using the cBioPortal. The transcriptional regulation of *FAT1* expression was investigated by chromatin immunoprecipitation (ChIP) and the luciferase reporter assays. In-cell western, Western blot and reverse transcription-quantitative polymerase chain reaction (RT-qPCR) were used to assess the indicated gene expression. In addition, colony formation and Transwell migration/invasion assays were employed to test cell proliferation, migration and invasion. Finally, RNA sequencing was used to study the transcriptomes.

Results: *FAT1* was frequently mutated in ESCC and was deleted in multiple cancers. Furthermore, the transcription factor E2F1 occupied the promoter region of *FAT1*, and depletion of E2F1 led to a decrease in transcription activity and mRNA levels of *FAT1*. Moreover, we found that knockdown of *FAT1* promoted KYSE30 and KYSE150 cell proliferation, migration and invasion; while overexpression of *FAT1* inhibited KYSE30 and KYSE410 cell proliferation, migration and invasion. In addition, knockdown of *FAT1* led to enrichment of the mitogen-activated protein kinase (MAPK) signaling pathway and cell adhesion process.

Conclusions: Our data provided evidence for the tumor suppressive function of *FAT1* in ESCC cells and elucidated the transcriptional regulation of *FAT1* by E2F1, which may facilitate the understanding of molecular mechanisms of the progression of ESCC.

Keywords: E2F1; ESCC; *FAT1*; tumor suppressor

Submitted Jan 25, 2019. Accepted for publication Apr 08, 2019.

doi: 10.21147/j.issn.1000-9604.2019.04.05

View this article at: <https://doi.org/10.21147/j.issn.1000-9604.2019.04.05>

Introduction

Worldwide, esophageal cancer is one of the most aggressive tumors, and is highly prevalent in China (1,2). It is the 4th leading cause of cancer-related mortality in China, where esophageal squamous cell carcinoma (ESCC) is the major histological type (3,4). There are advances in the early detection and treatment of patients with ESCC, but the 5-year survival of global ESCC patients is still very poor (5,6). Several large-scale analyses demonstrated that some genes and pathways, such as *TP53*, *RBI*, *CDKN2A*, *PIK3CA*, *Notch* and FAT atypical cadherin 1 (*FAT1*), may contribute to ESCC tumorigenesis (7-11). Among these aberrant genes, the “sleeping giant” (12) *FAT1* is inactivated by a two-hit model in ESCC tumors, where somatic mutations are often accompanied by the loss of heterozygosity or homozygous deletion (9,11), showing an anti-tumor activity (9,13,14). *FAT1* encodes a cadherin-like trans-membrane protein and regulates the cell-cell contact, polarization, migration and growth of mammalian cells (15-17). Interestingly, *FAT1* may function as both a tumor suppressor and an oncogene depending on different cell context (18-21). The inactivation of *FAT1* via somatic mutations or deletions is also observed in multiple human cancers to promote Wnt/ β -catenin signaling and tumorigenesis (18). Other mechanisms regulating *FAT1* expression remain poorly understood and need further investigation.

Transcriptional regulation by transcription factors is a critical way to affect gene expression. E2Fs are a large family of transcription factors that modulate gene expression by acting as either activators or repressors of transcription based on their structures and functions (22,23). In *Homo sapiens*, E2F transcription factor 1 (E2F1), which is the first member of the E2F family, is characterized as an activating transcription factor to mediate various biological processes, including cell cycle progression, apoptosis, DNA-damage response and metastasis (24-27). E2F1 binds to promoters of target genes, such as G1/S regulated genes and apoptosis-related genes, to regulate their expression (28-30), predominantly by interacting with the RB pocket protein (31). Advances in high-throughput technologies reveal that E2F1 also occupies a large fraction of gene promoters (32), suggesting that it has a wide spread regulation role in the human genome. However, the transcriptional regulation of E2F1

on the *FAT1* locus remains unknown.

In this study, we comprehensively analyzed the genetic alterations of *FAT1* in ESCC, as well as its copy number variants (CNVs) in other cancers. More importantly, the transcriptional regulation of *FAT1* by E2F1 was elaborated. In addition, the effects of *FAT1* on cell proliferation, migration and invasion were also monitored in ESCC cells. Finally, RNA sequencing (RNA-seq) was performed to investigate the gene expression profile upon *FAT1* knockdown.

Materials and methods

Cell lines

ESCC cell lines, KYSE30, KYSE150 and KYSE410, were generous gifts from Prof. Y Shimada of Kyoto University, Japan. All cell lines were cultured at 37 °C with 5% CO₂ in RPMI 1640 medium (Gibco) with 10% fetal bovine serum (FBS).

Cell transfection

Cells at the logarithmic growth phase were transfected with siRNAs or plasmids using Lipofectamine 2000 (Invitrogen, USA) according to the manufacturer's instructions. All siRNAs (25-mer duplex Stealth siRNAs) were obtained from Invitrogen, and the sequence information is as follows: siFAT1: HSS103568 and HSS176716 and siE2F1: HSS103016 and HSS103017. The FAT1-Trunc plasmid, which contains all key functional domains of FAT1 (18), was a generous gift from Dr. Luc GT Morris (Human Oncology and Pathogenesis Program, Memorial Sloan-Kettering Cancer Center).

Chromatin immunoprecipitation (ChIP)

Pierce Magnetic ChIP Kit (Thermo Fisher, Waltham, USA) was used according to the manufacturer's instructions. Briefly, KYSE30 cells were cross-linked with formaldehyde and the nucleus was isolated. Chromatin DNA was fragmented and incubated with E2F1 antibody (ab179445; Abcam, Cambridge, UK) followed by addition of magnetic beads. After washing and purification, the precipitated chromatins were analyzed by quantitative polymerase chain reaction (qPCR). The primers targeting

the *FAT1* promoter were synthesized by Invitrogen, and the sequences are as follows: forward 5'-GGAGCTCACCC GCCGTCTCA-3' and reverse 5'-GCTCGTGCGGC AGGTACCA-3'.

Luciferase reporter assay

To obtain the pGL3-*FAT1* vector, the promoter region of *FAT1*, ranging from -2000 bp to +500 bp, was synthesized and inserted into the pGL3-Basic vector by Generay (Shanghai, China). Then, KYSE30 cells were co-transfected by pGL3-*FAT1* vector and pRL-TK Renilla vector together with E2F1 siRNA. After 36 h of transfection, the luciferase activity was detected by the Dual-Luciferase Reporter Assay System (Promega, USA), and the Firefly luciferase activity was normalized to the Renilla luciferase activity.

RNA extraction and reverse transcription-quantitative polymerase chain reaction (RT-qPCR)

Total RNA from ESCC cells was purified using RNAiso plus (Takara, Dalian, China). Complementary DNA (cDNA) was synthesized from 1 µg of total RNA using a PrimeScript® RT reagent Kit with gDNA Eraser (Takara). TB Green® Premix Ex Taq® II kit (Takara) was used to detect the indicated RNA levels on the QuantStudio Real-Time PCR System (Applied Biosystems, USA) or the CFX96 Real-Time System (Bio-Rad, USA). The relative expression levels of the target genes were normalized to endogenous GAPDH. The primers synthesized by Invitrogen are listed in *Supplementary Table S1*.

Western blot

Total protein from ESCC cells was extracted using RIPA lysis buffer (Proteintech Group, Wuhan, China) that was supplemented with the protease inhibitor PMSF and was quantified by Enhanced BCA Protein Assay Kit (Beyotime Institute of Biotechnology, Shanghai, China) following the manufacturer's protocols. Equal quantities of proteins were separated by 10% SDS-PAGE and were transferred onto PVDF membranes. After blocking in 5% non-fat milk for 1 h, the membrane was then incubated with E2F1 primary antibody (ab179445; Abcam) at 4 °C overnight. Protein bands were detected using a horseradish-peroxidase (HRP)-conjugated IgG secondary antibody (Proteintech Group), and images were captured with the BioSpectrum imaging system (UVP, USA). GAPDH (60004-1-Ig; Proteintech Group) was used as loading control.

In-cell western assay

Cells grown in 96-well plates were fixed with 3.7% formaldehyde for 20 min and were permeabilized using 0.1% Triton X-100. After blocking with 5% non-fat milk for 1 h, cells were incubated with a mixture of *FAT1* primary antibody (ab190242; Abcam, UK) and GAPDH primary antibody (60004-1-Ig; Proteintech Group, China) overnight at 4 °C. Then, cells were washed with PBST and were incubated with 680 nm and 800 nm infrared-labeled secondary antibody solutions (LI-COR Biosciences, USA) for 1 h at room temperature. Fluorescent signals for *FAT1* and GAPDH were captured using the Odyssey infrared imaging system (LI-COR Biosciences, Lincoln, Nebraska, USA). Finally, the relative abundance of the *FAT1* protein was normalized to GAPDH.

Transwell migration/invasion assays

Transwell migration and invasion assays were performed using a Transwell plate (Corning, New York, USA) that was coated with (for invasion) or without (for migration) Matrigel Basement Membrane Matrix (BD). Briefly, 1.5×10^5 cells were seeded into the upper chamber of Transwell with serum-free medium, while culture medium with 20% FBS was added to the lower chamber. After culturing for 12–24 h, cells that migrated or invaded through the membrane were fixed with methanol for 10 min, stained with crystal violet solution for 5 min and finally photographed under a microscope (Leica, Germany).

Colony formation assay

A total of 1,000–3,000 transfected cells per well were seeded into plates containing medium with 10% FBS on d 0, and the cells were incubated at 37 °C with 5% CO₂ for 14 d. On d 14, the cells were washed with PBS, fixed with methanol for 10 min and then stained with crystal violet solution for another 10 min. After washing with water and drying at room temperature, the colonies were photographed and counted.

RNA sequencing (RNA-seq)

The transcriptome sequencing profiles of KYSE30-control and KYSE30-siFAT1 cells were obtained to detect the altered expression of downstream genes. Briefly, sequencing libraries were constructed with NEBNext Ultra RNA Library Prep Kit for Illumina (NEB, Ipswich, USA)

according to manufacturer's protocols. The libraries were sequenced on the Illumina HiSeq platform by Novogene (Beijing, China). Clean data were then mapped to the human reference genome hg19. The Fragments Per Kilobase of exon per Million mapped fragments (FPKM) of each gene was calculated and differential expression analysis was performed. The significantly differentially expressed genes between the control cells and the *FAT1* depleted cells were input to DAVID database (33,34) and enriched using Kyoto Encyclopedia of Genes and Genomes (KEGG) (35) and Gene Ontology (GO) analyses.

Statistical analysis

The data are presented as the $\bar{x} \pm s_{\bar{x}}$. $P < 0.05$ was considered statistically significant. The data were statistically analyzed using GraphPad Prism 6 (GraphPad Software, San Diego, CA, USA) by means of a two-sided Student's *t*-test.

Results

FAT1 exhibits a high frequency of genetic alterations in ESCC

To comprehensively explore the genetic alterations of *FAT1* in ESCC, we first analyzed the somatic mutations of *FAT1* from a study by Du *et al.* (36), which consisted of a total of 41 whole-genome sequences and 449 whole-exome sequences from seven published ESCC genomic data (7-10,37-39). We observed that *FAT1* was frequently mutated in ESCC (Figure 1A). The mutation rate of *FAT1* was 10% (49/490), and most of the mutations, including missense, truncating or inframe, occurred in the cadherin domains.

Furthermore, we analyzed the CNV features of *FAT1* in 154 ESCC patients from our previous studies (7,10) and found that CNVs of *FAT1* were altered in ESCC (Figure 1B). The total CNV rate, including the amplification of 1/154 (0.6%) and the deletion of 18/154 (11.7%), was

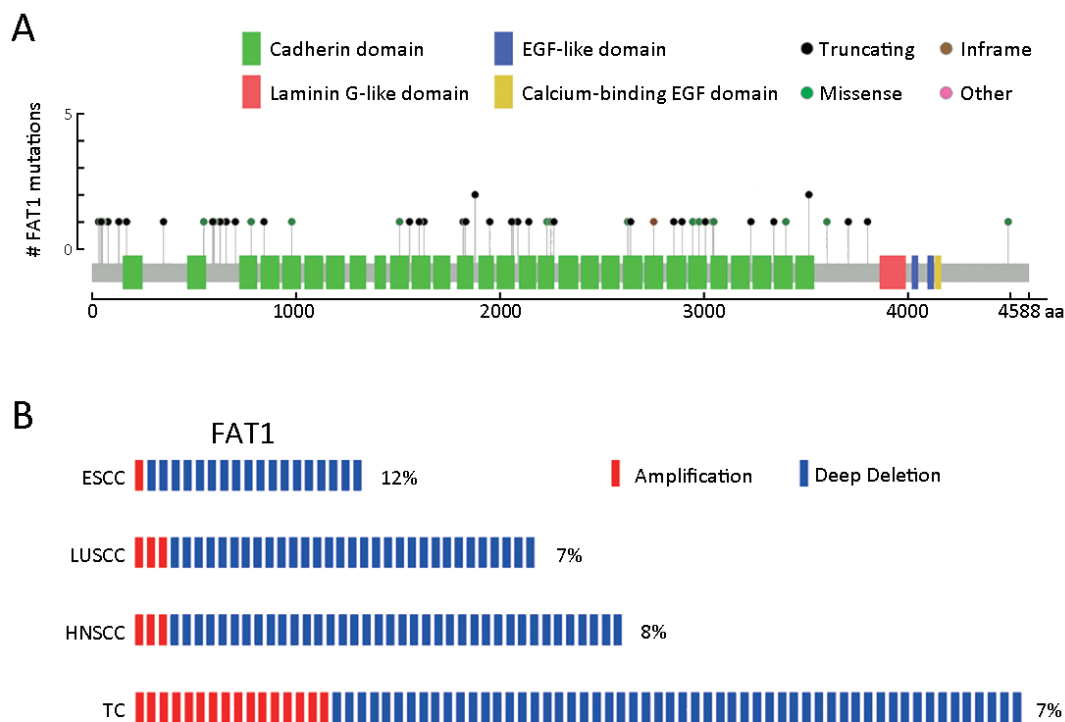


Figure 1 *FAT1* exhibits genetic alterations with high frequency in esophageal squamous cell carcinoma (ESCC). (A) Frequency of *FAT1* mutations in ESCC. Green box, cadherin domain; Red box, laminin G-like domain; Blue box, epidermal growth factor (EGF)-like domain; Yellow box, calcium-binding EGF domain; Black ball, truncating mutation; Green ball, missense mutation; Brown ball, inframe mutation; Pink ball, other mutation; (B) Frequency of *FAT1* copy number variants (CNVs) in three types of squamous cell carcinomas and tumor cell lines. The percentage represents the approximate ratio of CNVs. Red box, amplification; Blue box, deletion. LUSCC, lung squamous cell carcinoma; HNSCC, head and neck squamous cell carcinoma; TC, tumor cell lines.

approximately 12.3% (19/154). We also consulted The Cancer Genome Atlas (TCGA) database (40) and observed similar CNV features for *FAT1* in lung squamous cell carcinoma (LUSCC) and head and neck squamous cell carcinoma (HNSCC) using the cBioPortal (41,42) (Figure 1B). In LUSCC, the total CNV rate was approximately 6.8% (34/501), consisting of the amplification of 3/501 (0.6%) and the deletion of 31/501 (6.2%). Consistently, in HNSCC, the total CNV rate was approximately 7.9% (41/522), consisting of the amplification of 3/522 (0.6%) and the deletion of 38/522 (7.3%). In addition, we analyzed the CNV rate of *FAT1* in 995 tumor cell lines (TC) from the Cancer Cell Line Encyclopedia (CCLE) database (43) using the cBioPortal and found that the total CNV rate of *FAT1* in the pan tumor cell lines was approximately 7.2% (72/995), including the amplification of 16/995 (1.6%) and the deletion of 56/995 (5.6%) (Figure 1B). Taken together, our results revealed frequent inactivation of *FAT1* via mutations or deletions in ESCC and multiple other human cancers.

***FAT1* expression is regulated by transcription factor E2F1**

It is reported that *FAT1* expression is downregulated in ESCC tissues (9,13,14). In addition to the genetic alterations described above, we hypothesized that transcriptional regulation may also play an important role in this process. To test this, we consulted the encyclopedia of DNA elements (ENCODE) database (44) and observed a putative binding site for the transcription factor E2F1 on the promoter region of *FAT1* with the following identifiers: ENCFF000XCY, ENCFF000XEQ and ENCFF000ZLB (Figure 2A). Thus, a ChIP assay, using an E2F1 antibody, was then employed to confirm this occupancy. As expected, we observed a strong enrichment of E2F1 at the promoter region of *FAT1* when compared with that in IgG control (Figure 2B).

To ascertain whether E2F1 regulates the transcription of *FAT1*, we constructed a luciferase reporter, namely pGL3-FAT1, which contained the promoter region of *FAT1*. The luciferase activity of pGL3-FAT1 was much higher than the control vector upon transfection into KYSE30 cells,

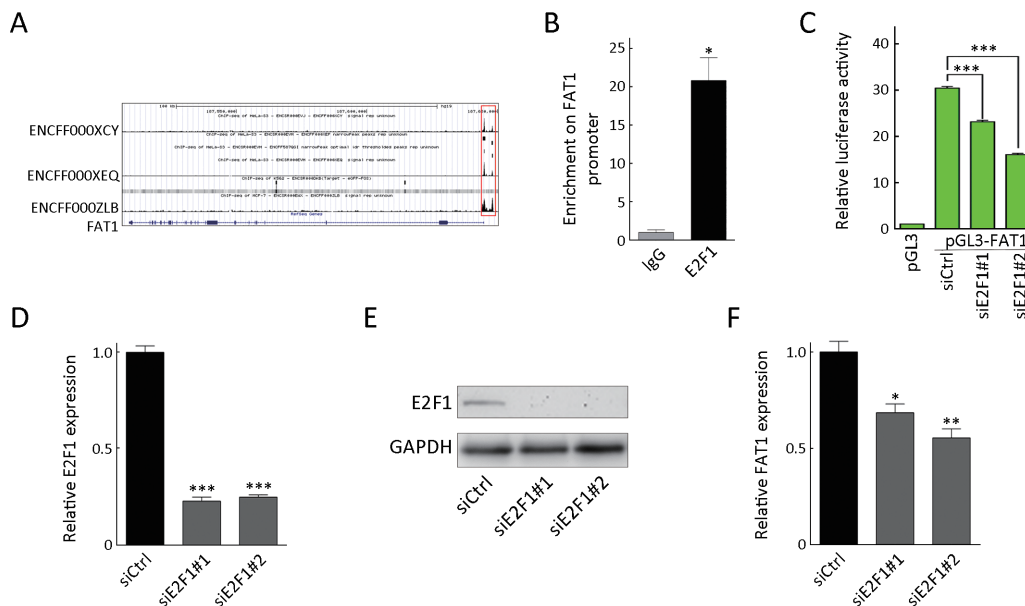


Figure 2 E2F1 regulates *FAT1* transcription. (A) Putative binding sites of E2F1 on the *FAT1* promoter region from different cohorts in encyclopedia of DNA elements (ENCODE) database. Red box represents binding reads of E2F1; (B) Enrichment of E2F1 on *FAT1* promoter in KYSE30 cells shown by chromatin immunoprecipitation (ChIP) and quantitative polymerase chain reaction (qPCR). Enrichment is determined as the amount of *FAT1* promoter associated to E2F1 relative to immunoglobulin G (IgG) control; (C) Luciferase activity of pGL3-FAT1 vector was measured in KYSE30 cells upon E2F1 knockdown. Data are presented as ratio of the firefly luciferase activity to Renilla luciferase activity; RT-qPCR (D) and Western blot (E) analyses of E2F1 expression in KYSE30 cells upon E2F1 knockdown. Relative RNA levels of E2F1 were normalized to endogenous GAPDH; (F) RT-qPCR analysis of *FAT1* expression in KYSE30 cells as described in (D). Relative RNA levels of *FAT1* were normalized to endogenous GAPDH. *, P<0.05; **, P<0.01; ***, P<0.001 vs. control.

and this increased luciferase activity was inhibited by siRNA-mediated E2F1 knockdown (Figure 2C). Meanwhile, knockdown of E2F1 reduced *FAT1* mRNA levels in KYSE30 cells (Figure 2F). The knockdown efficiency of E2F1 at the mRNA and protein levels was confirmed by RT-qPCR (Figure 2D) and Western blot (Figure 2E), respectively. Collectively, these results showed that E2F1 binds to the *FAT1* promoter to activate its transcription in ESCC cells.

Downregulation of *FAT1* promotes ESCC cell proliferation, migration and invasion

To explore the biological roles of *FAT1*, we performed a loss-of-function study using two small interfering RNAs (siRNAs) to knock down the *FAT1* in KYSE30 and KYSE150 cell lines. RT-qPCR and In-cell western assays showed that the two siRNAs effectively downregulated both mRNA and protein levels of *FAT1*, when compared with the control siRNA (Figure 3A,B). The colony formation and Transwell assays were used to elucidate the effects of *FAT1* knockdown on ESCC cell proliferation, migration and invasion. As shown in Figure 3C,D, the cells transfected with siRNAs targeting *FAT1* exhibited an enhanced colony formation ability compared with the control siRNA transfected cells. Taking advantage of the Transwell system, we validated that knockdown of *FAT1* enhanced the migration and invasion abilities of KYSE30

and KYSE150 cells (Figure 3E-H). Taken together, these results demonstrated that *FAT1* knockdown strengthened the aggressive potential of ESCC cells.

Overexpression of *FAT1* inhibits ESCC cell proliferation, migration and invasion

To test the gain-of-function of *FAT1* in ESCC cell lines, we transfected *FAT1* into KYSE30 and KYSE410 cell lines using an expression vector with all the key functional domains of *FAT1* (truncated *FAT1*, which was named *FAT1*-Trunc) (18). The mRNA and protein levels of *FAT1* were monitored by RT-qPCR and In-cell western assays, respectively (Figure 4A,B). *FAT1* overexpression reduced the colony formation abilities of KYSE30 and KYSE410 cells compared with the control empty vector (Figure 4C, D). Furthermore, the Transwell assays revealed that *FAT1* overexpression greatly attenuated the migration and invasion abilities of KYSE30 and KYSE410 cells (Figure 4E-H). Collectively, the results of both the loss-of-function and gain-of-function studies demonstrated that *FAT1* may act as a tumor suppressor in ESCC.

FAT1 is involved in mitogen-activated protein kinase (MAPK) signaling pathway and cell adhesion process in ESCC cells

To investigate the molecular mechanism of *FAT1* in ESCC

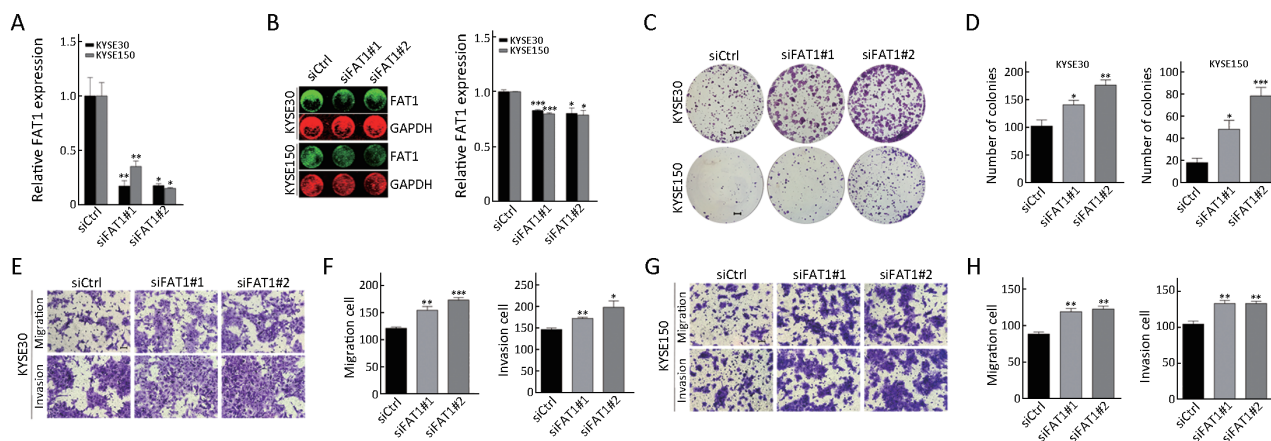


Figure 3 *FAT1* knockdown promotes KYSE30 and KYSE150 cell migration, invasion and proliferation. Reverse transcription-quantitative polymerase chain reaction (RT-qPCR) (A) and In-cell western analyses (B) of *FAT1* expression in KYSE30 and KYSE150 cells upon *FAT1* knockdown. Relative RNA and protein levels of *FAT1* were normalized to endogenous GAPDH; (C, D) KYSE30 and KYSE150 cells were transfected with the indicated siRNAs. After 24 h of transfection, cells were subject to colony formation assay. Representative results (C) and corresponding quantification (D) are shown (Scale bar = 2 mm); (E–H) Representative results of Transwell migration/invasion assays and corresponding quantification in KYSE30 (E, F) and KYSE150 (G, H) cells after transfected with indicated siRNAs as described in (C, D) (Scale bar = 100 μ m). *, $P < 0.05$; **, $P < 0.01$; ***, $P < 0.001$ vs. control.

oncogenesis, we performed a RNA-seq analysis using control and *FAT1* knocked-down KYSE30 cells, and subsequently analyzed the altered gene expression profiles (Supplementary Table S2). The KEGG pathway enrichment analysis revealed that upon *FAT1* knockdown, the significantly differentially expressed genes were enriched in multiple pathways, including the MAPK signaling pathway and cell adhesion molecules (CAMs) (Figure 5A). The GO functional analysis showed that these genes were enriched in biological processes, including the cell adhesion, cell-cell signaling and epidermis development (Figure 5B). Genes involved in the MAPK signaling pathway and the cell adhesion process were selected and validated by RT-qPCR after the knockdown of *FAT1* in KYSE30 cells. As expected, *FAT1* knockdown induced the mRNA levels of *MAP3K8*, *MAP2K2* and *MAP2K6* and decreased the mRNA level of MAPK inactivator *DUSP6* (Figure 5C). Meanwhile, *FAT1* knockdown enhanced the mRNA levels of *LICAM* and *CDH5*, which are involved in the cell adhesion process (Figure 5D). In conclusion, these results indicated that *FAT1* is involved in the MAPK signaling pathway and the cell adhesion process in ESCC cells.

Discussion

ESCC is one of the most prevalent malignant tumors in

China, with an elusive cancerogenesis and a poor prognosis (3,6). To study the molecular mechanism of ESCC tumorigenesis, several large-scale genomic sequencing studies have attempted to uncover the driving genomic variations (7-11). Interestingly, *FAT1* is frequently subject to inactivating mutations in ESCC (8-11), which is accompanied by loss of heterozygosity or homozygous deletion (9,11). Given that the case number of ESCC in each of these studies is relatively small, we analyzed the mutations of *FAT1* by using data that was combined from different cohorts by Du *et al.* (36) and revealed that *FAT1* was indeed frequently mutated in ESCC. Furthermore, we analyzed the *FAT1* CNV using our previous data (7,10) and databases, and the results showed a deletion of *FAT1* in ESCC and other cancers. Although the function of *FAT1* in tumorigenesis is still under debate in different types of tumors (18-21), it is considered a tumor suppressor gene in ESCC (9,13,14). Consistently, in this study, the *in vitro* experiments revealed that upregulation of *FAT1* inhibited ESCC cell proliferation, migration and invasion, while *FAT1* exhaustion resulted in the opposite effects. Thus, our study supplements the current theories that *FAT1* shows mutations and deletions in ESCC and acts as a tumor suppressor gene.

In addition to the dysregulation caused by the genetic alterations, an alternative possibility is that transcription is

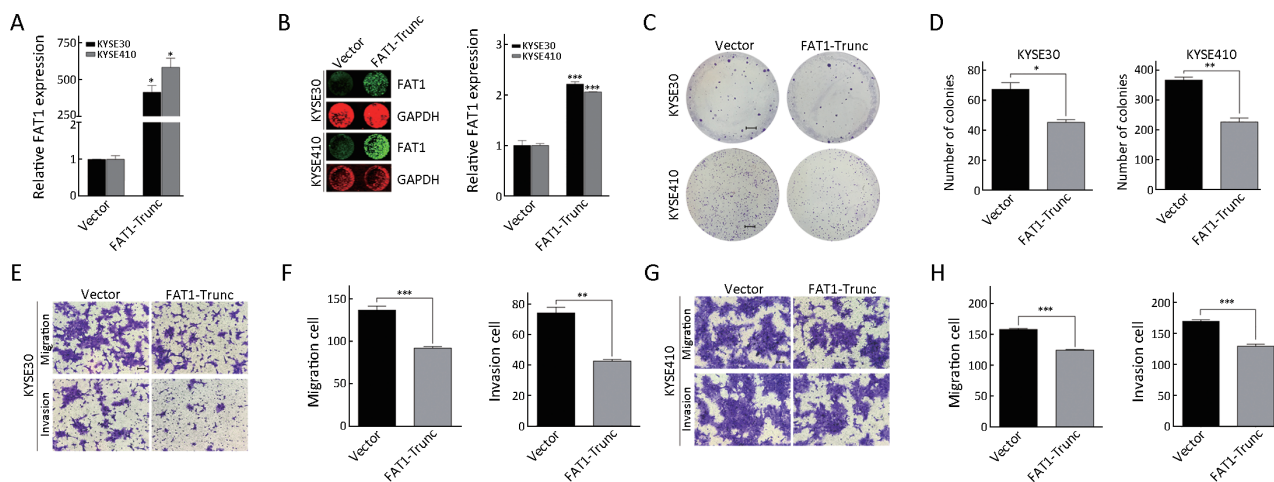


Figure 4 *FAT1* overexpression suppresses KYSE30 and KYSE410 cell proliferation, migration and invasion. Reverse transcription-quantitative polymerase chain reaction (RT-qPCR) (A) and In-cell western analyses (B) of *FAT1* expression in KYSE30 and KYSE410 cells upon *FAT1* overexpression. Relative RNA and protein levels of *FAT1* were normalized to endogenous GAPDH; (C, D) KYSE30 and KYSE410 cells were transfected with indicated vectors. After 24 h of transfection, cells were subject to colony formation assay. Representative results (C) and corresponding quantification (D) are shown (Scale bar =4 mm); (E–H) Representative results of Transwell migration/invasion assays and the corresponding quantification in KYSE30 (E, F) and KYSE410 (G, H) cells after transfected with the indicated vectors as described in (C, D) (Scale bar =100 μm). *, P<0.05; **, P<0.01; ***, P<0.001 vs. control.

changed during tumorigenesis. To illustrate the transcriptional regulation of *FAT1* mRNA expression in ESCC cells, we consulted the ENCODE database and found that the *FAT1* promoter region was occupied by transcription factor E2F1 in several ChIP-seq projects. E2F1 is an important transcription factor that regulates the gene expression in multiple types of human cancers and has both oncogenic and tumor-suppressive properties (45-48). Matrix metalloproteinase (*MMP*) genes are direct transcriptional targets of E2F1 in non-small cell lung cancer (NSCLC) cell lines (49). E2F1 binds to the promoter region of the phosphatase of activated cells 1 (*PAC1*) and activates its transcription in breast cancer cells (50). Nevertheless, little is known about the transcriptional regulatory effects of E2F1 in ESCC. Here, we characterized the binding and transcription activity of E2F1 upon the *FAT1* promoter region, as well as the influence of E2F1 on *FAT1* mRNA levels, and thus identified *FAT1* as a transcriptional target of E2F1 in ESCC cells.

The results of RNA-seq and RT-qPCR revealed that

FAT1 knockdown resulted in the altered expression of package of genes that are involved in the MAPK signaling pathway, which is consistent with previous report (13). The MAPK signaling pathway is an important signaling component that consists of a set of evolutionarily conserved kinase cascades from yeast to human, including MAPK kinase kinase (MKKK), MAPK kinase kinase (MKK) and MAPK (51,52). It is reported that the MAPK pathway is dysregulated in ESCC and may function as an oncogene in ESCC tumorigenesis (53,54). On the other hand, the GO functional analysis and RT-qPCR also revealed that loss of *FAT1* subsequently upregulated the expression of genes that participate in the cell adhesion process, including *LICAM* and *CHD5*, which may play roles in the progression or metastasis of multiple cancers and correlate with poor outcomes (55-58). Collectively, the RNA-seq results revealed that *FAT1* knockdown led to the abnormal expression of genes in the MAPK signaling pathway and cell adhesion process, further indicating that *FAT1* is involved in ESCC tumorigenesis

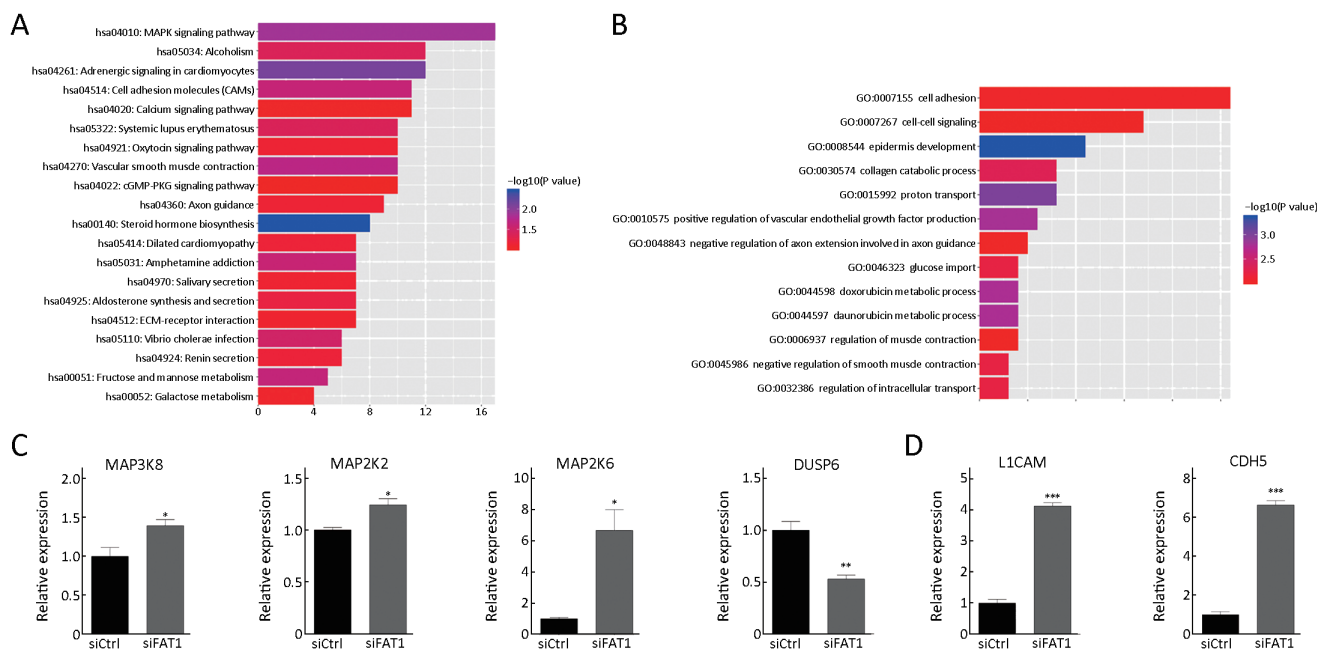


Figure 5 Global transcriptional identification of genes regulated by *FAT1*. KYSE30 cells were transfected with *FAT1* siRNA or scramble control siRNA. After 48 h of transfection, cells were collected and subject to RNA-seq. Kyoto Encyclopedia of Genes and Genomes (KEGG) pathway enrichment analysis (A) and Gene Ontology (GO) functional analysis (B) of significantly differently expressed genes upon *FAT1* knockdown in KYSE30 cells; Reverse transcription-quantitative polymerase chain reaction (RT-qPCR) showing the expression of genes involved in mitogen-activated protein kinase (MAPK) signal pathway (C) and cell adhesion process in KYSE30 cells after 48 h of transfection with the indicated siRNAs (D). Relative RNA levels of genes were normalized to endogenous GAPDH. *, $P < 0.05$; **, $P < 0.01$; ***, $P < 0.001$ vs. control.

Conclusions

In this study we identified *FAT1* as the transcriptional target of E2F1. Moreover, we also validated that *FAT1* exhibits tumor suppressive function in ESCC and participates in the MAPK signaling pathway and cell adhesion process. These results advance our understanding of mechanisms by which *FAT1* is inactive and regulated in ESCC, and the data also highlight the importance of *FAT1* in ESCC tumorigenesis.

Acknowledgements

This work was supported by the National Basic Research Program of China (973 Program) (No. 2015CB553906 and 2015CB553904), the National Natural Science Foundation of China (No. 81490753 and 81830086) and the Education Department of Liaoning Province in China (Scientific Research Projects, No. L2016038).

Footnote

Conflicts of Interest: The authors have no conflicts of interests to declare.

References

1. Bray F, Ferlay J, Soerjomataram I, et al. Global cancer statistics 2018: GLOBOCAN estimates of incidence and mortality worldwide for 36 cancers in 185 countries. *CA Cancer J Clin* 2018;68:394-424.
2. Arnold M, Soerjomataram I, Ferlay J, et al. Global incidence of oesophageal cancer by histological subtype in 2012. *Gut* 2015;64:381-7.
3. Chen W, Zheng R, Baade PD, et al. Cancer statistics in China, 2015. *CA Cancer J Clin* 2016;66:115-32.
4. Yang Z, Zeng H, Xia R, et al. Annual cost of illness of stomach and esophageal cancer patients in urban and rural areas in China: A multi-center study. *Chin J Cancer Res* 2018;30:439-48.
5. Ohashi S, Miyamoto S, Kikuchi O, et al. Recent advances from basic and clinical studies of esophageal squamous cell carcinoma. *Gastroenterology* 2015;149:1700-15.
6. Pennathur A, Gibson MK, Jobe BA, et al. Oesophageal carcinoma. *Lancet* 2013;381:400-12.
7. Song Y, Li L, Ou Y, et al. Identification of genomic alterations in oesophageal squamous cell cancer. *Nature* 2014;509:91-5.
8. Gao YB, Chen ZL, Li JG, et al. Genetic landscape of esophageal squamous cell carcinoma. *Nat Genet* 2014;46:1097-102.
9. Lin DC, Hao JJ, Nagata Y, et al. Genomic and molecular characterization of esophageal squamous cell carcinoma. *Nat Genet* 2014;46:467-73.
10. Zhang L, Zhou Y, Cheng C, et al. Genomic analyses reveal mutational signatures and frequently altered genes in esophageal squamous cell carcinoma. *Am J Hum Genet* 2015;96:597-611.
11. Sawada G, Niida A, Uchi R, et al. Genomic landscape of esophageal squamous cell carcinoma in a Japanese population. *Gastroenterology* 2016;150:1171-82.
12. Sadeqzadeh E, de Bock CE, Thorne RF. Sleeping giants: emerging roles for the fat cadherins in health and disease. *Med Res Rev* 2014;34:190-221.
13. Hu X, Zhai Y, Kong P, et al. FAT1 prevents epithelial mesenchymal transition (EMT) via MAPK/ERK signaling pathway in esophageal squamous cell cancer. *Cancer Lett* 2017;397:83-93.
14. Hu X, Zhai Y, Shi R, et al. FAT1 inhibits cell migration and invasion by affecting cellular mechanical properties in esophageal squamous cell carcinoma. *Oncol Rep* 2018;39:2136-46.
15. Tanoue T, Takeichi M. Mammalian Fat1 cadherin regulates actin dynamics and cell-cell contact. *J Cell Biol* 2004;165:517-28.
16. Moeller MJ, Soofi A, Braun GS, et al. Protocadherin FAT1 binds Ena/VASP proteins and is necessary for actin dynamics and cell polarization. *EMBO J* 2004;23:3769-79.
17. Hou R, Liu L, Anees S, et al. The Fat1 cadherin integrates vascular smooth muscle cell growth and migration signals. *J Cell Biol* 2006;173:417-29.
18. Morris LG, Kaufman AM, Gong Y, et al. Recurrent somatic mutation of FAT1 in multiple human cancers leads to aberrant Wnt activation. *Nat Genet* 2013;45:253-61.
19. Valletta D, Czech B, Spruss T, et al. Regulation and function of the atypical cadherin FAT1 in hepatocellular carcinoma. *Carcinogenesis* 2014;35:1407-15.
20. Dikshit B, Irshad K, Madan E, et al. FAT1 acts as an upstream regulator of oncogenic and inflammatory pathways, via PDCD4, in glioma cells. *Oncogene*

- 2013;32:3798-808.
21. de Bock CE, Ardjmand A, Molloy TJ, et al. The Fat1 cadherin is overexpressed and an independent prognostic factor for survival in paired diagnosis-relapse samples of precursor B-cell acute lymphoblastic leukemia. *Leukemia* 2012;26:918-26.
 22. Trimarchi JM, Lees JA. Sibling rivalry in the E2F family. *Nat Rev Mol Cell Biol* 2002;3:11-20.
 23. Iaquinta PJ, Lees JA. Life and death decisions by the E2F transcription factors. *Curr Opin Cell Biol* 2007;19:649-57.
 24. Castillo DS, Campalans A, Belluscio LM, et al. E2F1 and E2F2 induction in response to DNA damage preserves genomic stability in neuronal cells. *Cell Cycle* 2015;14:1300-14.
 25. Johnson DG, Schwarz JK, Cress WD, et al. Expression of transcription factor E2F1 induces quiescent cells to enter S phase. *Nature* 1993;365:349-52.
 26. Qin XQ, Livingston DM, Kaelin WG, Jr., et al. Deregulated transcription factor E2F-1 expression leads to S-phase entry and p53-mediated apoptosis. *Proc Natl Acad Sci U S A* 1994;91:10918-22.
 27. Hollern DP, Honeysett J, Cardiff RD, et al. The E2F transcription factors regulate tumor development and metastasis in a mouse model of metastatic breast cancer. *Mol Cell Biol* 2014;34:3229-43.
 28. Nahle Z, Polakoff J, Davuluri RV, et al. Direct coupling of the cell cycle and cell death machinery by E2F. *Nat Cell Biol* 2002;4:859-64.
 29. Gomez-Manzano C, Mitlianga P, Fueyo J, et al. Transfer of E2F-1 to human glioma cells results in transcriptional up-regulation of Bcl-2. *Cancer Res* 2001;61:6693-7.
 30. Bertoli C, Skotheim JM, de Bruin RA. Control of cell cycle transcription during G1 and S phases. *Nat Rev Mol Cell Biol* 2013;14:518-28.
 31. Dick FA, Rubin SM. Molecular mechanisms underlying RB protein function. *Nat Rev Mol Cell Biol* 2013;14:297-306.
 32. Bieda M, Xu X, Singer MA, et al. Unbiased location analysis of E2F1-binding sites suggests a widespread role for E2F1 in the human genome. *Genome Res* 2006;16:595-605.
 33. Huang da W, Sherman BT, Lempicki RA. Bioinformatics enrichment tools: paths toward the comprehensive functional analysis of large gene lists. *Nucleic Acids Res* 2009;37:1-13.
 34. Huang da W, Sherman BT, Lempicki RA. Systematic and integrative analysis of large gene lists using DAVID bioinformatics resources. *Nat Protoc* 2009;4:44-57.
 35. Kanehisa M, Sato Y, Furumichi M, et al. New approach for understanding genome variations in KEGG. *Nucleic Acids Res* 2019;47:D590-D595.
 36. Du P, Huang P, Huang X, et al. Comprehensive genomic analysis of oesophageal squamous cell carcinoma reveals clinical relevance. *Sci Rep* 2017;7:15324.
 37. Cancer Genome Atlas Research Network, Analysis Working Group: Asan University, BC Cancer Agency, et al. Integrated genomic characterization of oesophageal carcinoma. *Nature* 2017;541:169-175.
 38. Qin HD, Liao XY, Chen YB, et al. Genomic characterization of esophageal squamous cell carcinoma reveals critical genes underlying tumorigenesis and poor prognosis. *Am J Hum Genet* 2016;98:709-27.
 39. Agrawal N, Jiao Y, Bettegowda C, et al. Comparative genomic analysis of esophageal adenocarcinoma and squamous cell carcinoma. *Cancer Discov* 2012;2:899-905.
 40. Cancer Genome Atlas Research Network, Weinstein JN, Collisson EA, et al. The Cancer Genome Atlas Pan-Cancer analysis project. *Nat Genet* 2013;45:1113-20.
 41. Gao J, Aksoy BA, Dogrusoz U, et al. Integrative analysis of complex cancer genomics and clinical profiles using the cBioPortal. *Sci Signal* 2013;6:pl1.
 42. Cerami E, Gao J, Dogrusoz U, et al. The cBio cancer genomics portal: an open platform for exploring multidimensional cancer genomics data. *Cancer Discov* 2012;2:401-4.
 43. Barretina J, Caponigro G, Stransky N, et al. The Cancer Cell Line Encyclopedia enables predictive modelling of anticancer drug sensitivity. *Nature* 2012;483:603-7.
 44. Consortium ENCODE Project. An integrated encyclopedia of DNA elements in the human genome. *Nature* 2012;489:57-74.
 45. Yamasaki L, Bronson R, Williams BO, et al. Loss of E2F-1 reduces tumorigenesis and extends the lifespan

- of Rb1(+/-)mice. *Nat Genet* 1998;18:360-4.
46. Russell JL, Weaks RL, Berton TR, et al. E2F1 suppresses skin carcinogenesis via the ARF-p53 pathway. *Oncogene* 2006;25:867-76.
 47. Yamasaki L, Jacks T, Bronson R, et al. Tumor induction and tissue atrophy in mice lacking E2F-1. *Cell* 1996;85:537-48.
 48. Conner EA, Lemmer ER, Omori M, et al. Dual functions of E2F-1 in a transgenic mouse model of liver carcinogenesis. *Oncogene* 2000;19:5054-62.
 49. Johnson JL, Pillai S, Pernazza D, et al. Regulation of matrix metalloproteinase genes by E2F transcription factors: Rb-Raf-1 interaction as a novel target for metastatic disease. *Cancer Res* 2012;72:516-26.
 50. Wu J, Jin YJ, Calaf GM, et al. PAC1 is a direct transcription target of E2F-1 in apoptotic signaling. *Oncogene* 2007;26:6526-35.
 51. Burotto M, Chiou VL, Lee JM, et al. The MAPK pathway across different malignancies: a new perspective. *Cancer* 2014;120:3446-56.
 52. Cargnello M, Roux PP. Activation and function of the MAPKs and their substrates, the MAPK-activated protein kinases. *Microbiol Mol Biol Rev* 2011;75:50-83.
 53. Qin X, Zheng S, Liu T, et al. Roles of phosphorylated JNK in esophageal squamous cell carcinomas of Kazakh ethnic. *Mol Carcinog* 2014;53:526-36.
 54. Gavine PR, Wang M, Yu D, et al. Identification and validation of dysregulated MAPK7 (ERK5) as a novel oncogenic target in squamous cell lung and esophageal carcinoma. *BMC Cancer* 2015;15:454.
 55. Guo JC, Xie YM, Ran LQ, et al. L1CAM drives oncogenicity in esophageal squamous cell carcinoma by stimulation of ezrin transcription. *J Mol Med (Berl)* 2017;95:1355-1368.
 56. Higuchi K, Inokuchi M, Takagi Y, et al. Cadherin 5 expression correlates with poor survival in human gastric cancer. *J Clin Pathol* 2017;70:217-221.
 57. Tischler V, Pfeifer M, Hausladen S, et al. L1CAM protein expression is associated with poor prognosis in non-small cell lung cancer. *Mol Cancer* 2011;10:127.
 58. Fry SA, Sinclair J, Timms JF, et al. A targeted glycoproteomic approach identifies cadherin-5 as a novel biomarker of metastatic breast cancer. *Cancer Lett* 2013;328:335-44.

Cite this article as: Wang Y, Wang G, Ma Y, Teng J, Wang Y, Cui Y, Dong Y, Shao S, Zhan Q, Liu X. *FAT1*, a direct transcriptional target of E2F1, suppresses cell proliferation, migration and invasion in esophageal squamous cell carcinoma. *Chin J Cancer Res* 2019;31(4):609-619. doi: 10.21147/j.issn.1000-9604.2019.04.05

Table S1 Primer sequences for RT-qPCR

Primer	Sequences
GAPDH-F	GGTCATCCATGACAACCTTTGGTATC
GAPDH-R	GTAGAGGCAGGGATGATGTTCTG
FAT1-F	GGTCCAGATCGAGGCATTTGA
FAT1-R	TCATCTTGCTGTTCTCGGTCTAG
FAT1-Trunc-F	GGCGTTTGGATCTGCTGAGTA
FAT1-Trunc-R	GTCTCTGAGCTCCTTCCAGTC
E2F1-F	GCTGGACCTGGAAACTGACC
E2F1-R	TCATAGCGTGACTTCTCCCCC
MAP3K8-F	CCGGGCAGTCTCTTTCTGTT
MAP3K8-R	GCTCTGCCCCCTGACTCAC
MAP2K2-F	TATTGTGAACGAGCCACCTCC
MAP2K2-R	TTACACAACCAGCCGGCAAA
MAP2K6-F	GCCGAAGTGTGGTCTTTGGA
MAP2K6-R	CTGCAGTTCGCTTACTTGCC
DUSP6-F	ATGGACCGACTGTACCGTGT
DUSP6-R	ACATGTGGCTGTCATCTTGGT
L1CAM-F	ATCATCCTCCTGCTCCTCGT
L1CAM-R	TCTCCAGGGACCTGACTCG
CDH5-F	ATGAGATCGTGGTGGAAAGCG
CDH5-R	ATGTGTACTIONGGTCTGGGTGA

RT-qPCR, reverse transcription-quantitative polymerase chain reaction; F, forward primer; R, reverse primer.

Table S2 Top 100 significantly differentially expressed genes ($P < 0.05$) in *FAT1* knocked-down KYSE30 cells

Gene ID	Gene_name	Gene_locus	siFAT_FPKM	siCtrl_FPKM	Log2 fold change	P	Padj
ENSG00000172062	<i>SMN1</i>	5:70220768–70249769	5.409958	51.32826	-3.25018	9.20E-13	2.11E-08
ENSG00000228589	<i>SPCS2P4</i>	1:28421582–28422933	1.704209	16.4227	-3.27085	5.89E-12	6.76E-08
ENSG00000094755	<i>GABRP</i>	5:170190354–170241051	2.248404	0.139269	3.985165	3.52E-10	2.69E-06
ENSG00000233013	<i>FAM157B</i>	9:141106637–141143444	0.141909	1.719214	-3.58454	2.44E-09	1.40E-05
ENSG00000144857	<i>BOC</i>	3:112929850–113006303	1.273603	0.11785	3.411765	2.95E-08	0.000136
ENSG00000226054	<i>MEMO1P1</i>	21:37502669–37504208	10.44055	1.85337	2.48752	6.49E-08	0.000237
ENSG00000180673	<i>EXOC5P1</i>	4:63682544–63684512	0.553869	0.013287	5.217273	7.22E-08	0.000237
ENSG00000114854	<i>TNNC1</i>	3:52485118–52488086	2.043411	0.088238	4.448301	1.15E-07	0.00033
ENSG00000188199	<i>NUTM2B</i>	10:81462983–81474437	0.40364	0.017786	4.419231	1.52E-07	0.000387
ENSG00000272343	<i>RP11-140I16.3</i>	8:57135247–57135732	1.495978	0	7.856664	7.40E-07	0.0017
ENSG00000169627	<i>BOLA2B</i>	16:30204255–30205627	6.462627	28.7566	-2.15757	1.28E-06	0.002682
ENSG00000251070	<i>BMS1P6</i>	10:48187416–48199256	0.491616	0	7.705352	2.40E-06	0.0046
ENSG00000225465	<i>RFPL1S</i>	22:29832818–29874164	0.526845	0.058036	3.147156	8.67E-06	0.015322
ENSG00000009724	<i>MASP2</i>	1:11086580–11107290	0.63512	0.05413	3.496074	1.26E-05	0.020666
ENSG00000139899	<i>CBLN3</i>	14:24895738–24900160	0.806774	0.102465	2.947334	1.47E-05	0.021116
ENSG00000166268	<i>MYRFL</i>	12:70219084–70352877	0.398282	0.026058	3.850765	1.47E-05	0.021116
ENSG00000147573	<i>TRIM55</i>	8:67039131–67087720	0.012702	0.356515	-4.646	1.58E-05	0.021279
ENSG00000186442	<i>KRT3</i>	12:53183469–53189901	0.565061	0.079075	2.811247	1.83E-05	0.022482

Table S2 (continued)

Table S2 (continued)

Gene ID	Gene_name	Gene_locus	siFAT_FPKM	siCtrl_FPKM	Log2 fold change	P	Padj
ENSG00000183783	<i>KCTD8</i>	4:44175926-44450824	0.349388	0	7.411466	1.96E-05	0.022482
ENSG00000237938	<i>RP11-288I21.1</i>	1:16049214-16063391	0.826615	0	7.411466	1.96E-05	0.022482
ENSG00000152726	<i>FAM21B</i>	10:47894023-47949412	0.219917	1.016119	-2.20698	2.83E-05	0.030915
ENSG00000130635	<i>COL5A1</i>	9:137533620-137736686	2.739808	0.699106	1.963217	3.32E-05	0.033136
ENSG00000109511	<i>ANXA10</i>	4:169013666-169108841	0.025271	0.654749	-4.53108	3.37E-05	0.033136
ENSG00000197409	<i>HIST1H3D</i>	6:26197068-26199521	3.076838	0.574103	2.407265	3.46E-05	0.033136
ENSG00000020181	<i>GPR124</i>	8:37641709-37702414	0.360846	0.056548	2.652953	3.61E-05	0.033166
ENSG00000271815	<i>CTD-2235C13.3</i>	5:74659585-74660067	0	0.975007	-7.23828	4.78E-05	0.042186
ENSG00000198576	<i>ARC</i>	8:143692405-143696833	0.589737	0.096098	2.594743	5.29E-05	0.044146
ENSG00000174498	<i>IGDCC3</i>	15:65619465-65670378	1.223256	0.248577	2.285585	5.38E-05	0.044146
ENSG00000183793	<i>NPIPA5</i>	16:15457516-15474904	0.177824	1.234089	-2.77703	5.82E-05	0.045299
ENSG00000150165	<i>ANXA8L1</i>	10:47157983-47174093	0.408894	1.765685	-2.1097	5.92E-05	0.045299
ENSG00000202198	<i>RN7SK</i>	6:52860418-52860748	4.539458	0.790414	2.50285	7.11E-05	0.048664
ENSG00000037280	<i>FLT4</i>	5:180028506-180076624	0.010123	0.240426	-4.4062	7.35E-05	0.048664
ENSG00000236617	<i>RP11-46H11.12</i>	12:133464428-133465169	1.047994	0.04714	4.314013	7.35E-05	0.048664
ENSG00000255967	<i>RP11-438L7.3</i>	12:8786963-8790204	0.254545	0.01145	4.314013	7.35E-05	0.048664
ENSG00000259804	<i>CTD-2012K14.7</i>	16:67595314-67596212	0.512194	0	7.2013	7.55E-05	0.048664
ENSG00000259243	<i>GOLGA6L19</i>	15:83011379-83018198	0.750822	0.090061	3.017247	7.63E-05	0.048664
ENSG00000183578	<i>TNFAIP8L3</i>	15:51348795-51397473	0.299989	0.023132	3.614736	8.17E-05	0.049821
ENSG00000101222	<i>SPEF1</i>	20:3758151-3762095	0.597876	0.090061	2.701856	8.24E-05	0.049821
ENSG00000269990	<i>CTD-3074O7.12</i>	11:66303369-66305407	2.008676	0.538908	1.890325	0.000104	0.060948
ENSG00000083857	<i>FAT1</i>	4:187508937-187647876	43.28378	133.7042	-1.63191	0.000107	0.061382
ENSG00000269054	<i>CTD-2619J13.3</i>	19:58873951-58877958	0.705572	0.033117	4.252951	0.00011	0.061382
ENSG00000233337	<i>UBE2FP3</i>	1:111980136-111980659	0	0.798861	-7.06955	0.00012	0.063304
ENSG00000273156	<i>RP11-127B20.2</i>	4:83266029-83266693	0.655981	0	7.123842	0.00012	0.063304
ENSG00000245711	<i>NADK2-AS1</i>	5:36221157-36222004	0.168298	1.308135	-2.931	0.000121	0.063304
ENSG00000205683	<i>DPF3</i>	14:73086004-73360809	0.207135	1.024892	-2.29923	0.000127	0.064657
ENSG00000169174	<i>PCSK9</i>	1:55505221-55530525	2.306266	0.668728	1.779379	0.000135	0.067382
ENSG00000261597	<i>RP11-353B9.1</i>	15:49944336-49948429	0.023678	0.204496	-3.07449	0.000138	0.067382
ENSG00000111341	<i>MGP</i>	12:15034115-15038860	36.15032	11.74596	1.616772	0.000157	0.073872
ENSG00000174194	<i>AGAP8</i>	10:51224681-51371321	0.900366	0.161998	2.452153	0.000163	0.073872
ENSG00000174521	<i>TTC9B</i>	19:40721965-40724306	0.015309	0.330546	-4.26948	0.000164	0.073872
ENSG00000236431	<i>AC009237.11</i>	2:96201865-96202243	1.406772	0.069031	4.189189	0.000164	0.073872
ENSG00000088053	<i>GP6</i>	19:55525073-55549632	0.371744	0.03087	3.508334	0.000167	0.073872
ENSG00000169583	<i>CLIC3</i>	9:139889087-139891255	29.72199	9.6876	1.612147	0.000177	0.076852
ENSG00000214940	<i>NPIPA8</i>	16:18411799-18441131	0.291042	1.135932	-1.96402	0.000191	0.0811
ENSG00000112541	<i>PDE10A</i>	6:165740776-166400091	0.541212	1.73594	-1.68501	0.000196	0.081985
ENSG00000179044	<i>EXOC3L1</i>	16:67218269-67224107	0.556412	0.083427	2.703749	0.000211	0.085184
ENSG00000260604	<i>RP1-140K8.5</i>	6:3905144-3912213	0.123402	0.018503	2.703749	0.000211	0.085184
ENSG00000234231	<i>AC093616.4</i>	2:88000503-88038766	0.638541	2.228317	-1.8048	0.000228	0.087622
ENSG00000102385	<i>DRP2</i>	X:100474758-100519486	0.007813	0.096993	-3.55545	0.000241	0.087622
ENSG00000136449	<i>MYCBPAP</i>	17:48585745-48608862	0.037028	0.459696	-3.55545	0.000241	0.087622
ENSG00000222020	<i>AC062017.1</i>	2:240323130-240324058	0.115956	1.439574	-3.55545	0.000241	0.087622
ENSG00000269896	<i>RP4-740C4.6</i>	1:2281853-2284259	0.815548	0.19565	2.047422	0.000244	0.087622

Table S2 (continued)

Table S2 (continued)

Gene ID	Gene_name	Gene_locus	siFAT_FPKM	siCtrl_FPKM	Log2 fold change	P	Padj
ENSG00000177694	<i>NAALADL2</i>	3:174156363–175523428	0.849999	0.149379	2.483511	0.000246	0.087622
ENSG00000166592	<i>RRAD</i>	16:66955582–66959547	0.550792	0.028315	4.122478	0.000248	0.087622
ENSG00000268650	<i>AC068499.10</i>	19:18315540–18331290	0.994008	0.051099	4.122478	0.000248	0.087622
ENSG00000144583	<i>4-Mar</i>	2:217122588–217236750	0.877403	2.64745	-1.59731	0.000276	0.094002
ENSG00000263320	<i>RP11-498D10.6</i>	16:71963914–71965102	0.713389	0.11002	2.663255	0.00028	0.094002
ENSG00000180596	<i>HIST1H2BC</i>	6:26115101–26124154	12.72822	4.083932	1.633976	0.000291	0.094002
ENSG00000090661	<i>CERS4</i>	19:8271620–8327305	3.35701	0.968069	1.786044	0.000292	0.094002
ENSG00000261655	<i>CTD-3064M3.3</i>	8:142363503–142365465	0.345683	0.039984	3.057257	0.0003	0.094002
ENSG00000146070	<i>PLA2G7</i>	6:46671938–46703430	0.222066	0	6.862874	0.000315	0.094002
ENSG00000164509	<i>IL31RA</i>	5:55147207–55218678	0	0.160836	-6.97715	0.000315	0.094002
ENSG00000223979	<i>SMCR2</i>	17:17577340–17581002	0.644544	0	6.862874	0.000315	0.094002
ENSG00000255585	<i>RP11-188C12.2</i>	9:140682117–140683139	0.35535	0	6.862874	0.000315	0.094002
ENSG00000269846	<i>RBL1</i>	20:35724188–35725581	0	0.281521	-6.97715	0.000315	0.094002
ENSG00000269903	<i>RP11-571M6.18</i>	12:58208277–58208709	0	0.906329	-6.97715	0.000315	0.094002
ENSG00000271803	<i>RP1-63M2.5</i>	20:32262323–32263186	0.826188	0	6.862874	0.000315	0.094002
ENSG00000260051	<i>LA16c-390E6.4</i>	16:1501761–1502654	0.425173	2.019576	-2.23803	0.000333	0.097904
ENSG00000142920	<i>ADC</i>	1:33546705–33586131	0.950682	0.211778	2.151327	0.000338	0.098341
ENSG00000228137	<i>AP001469.7</i>	21:47666804–47667596	1.491375	0.134168	3.393454	0.000349	0.098807
ENSG00000253559	<i>OSGEPL1-AS1</i>	2:190627430–190630282	1.077104	0.096899	3.393454	0.000349	0.098807
ENSG00000120738	<i>EGR1</i>	5:137801179–137805004	4.139541	1.392342	1.566469	0.000355	0.099482
ENSG00000169282	<i>KCNAB1</i>	3:155755490–156256545	0.595795	0.094587	2.621592	0.000372	0.102948
ENSG00000269951	<i>RP11-797A18.6</i>	15:77359996–77360667	0.036064	0.700786	-4.11843	0.000377	0.102948
ENSG00000171873	<i>ADRA1D</i>	20:4201329–4229721	2.924115	0.967541	1.589637	0.000406	0.109612
ENSG00000121966	<i>CXCR4</i>	2:136871919–136875735	0.158022	0.713387	-2.16617	0.000416	0.109612
ENSG00000262691	<i>CTC-277H1.7</i>	16:67295011–67297687	0.244431	0.029319	3.005036	0.000419	0.109612
ENSG00000263740	<i>RN7SL4P</i>	3:15780022–15780315	1.813492	6.852133	-1.91633	0.00042	0.109612
ENSG00000134258	<i>VTCN1</i>	1:117686209–117753556	17.60335	6.175808	1.50607	0.000425	0.109728
ENSG00000163623	<i>NKX6-1</i>	4:85413140–85419603	0.743832	0.184474	1.999144	0.000444	0.113408
ENSG00000235169	<i>SMIM1</i>	1:3689352–3692546	3.280273	0.792809	2.035269	0.000462	0.116388
ENSG00000224419	<i>KRT18P27</i>	13:90882638–90883936	0.074626	0.563938	-2.88262	0.000466	0.116388
ENSG00000271780	<i>RP11-1017G21.5</i>	14:102414684–102415762	0.112302	0.751662	-2.71604	0.000495	0.121711
ENSG00000247627	<i>MTND4P12</i>	5:134262350–134263726	1.777574	5.281938	-1.57473	0.000503	0.121711
ENSG00000167588	<i>GPD1</i>	12:50497602–50505102	0.480519	0.045108	3.332392	0.000507	0.121711
ENSG00000215912	<i>TTC34</i>	1:2567415–2718286	0	0.173674	-6.87843	0.000517	0.121711
ENSG00000273448	<i>RP11-166O4.6</i>	7:66798034–66799370	0.253768	0	6.764224	0.000517	0.121711
ENSG00000253570	<i>RNF5P1</i>	8:38458179–38458718	0.314155	1.792629	-2.49545	0.000519	0.121711
ENSG00000255248	<i>RP11-166D19.1</i>	11:121899063–121987031	0.374941	1.379889	-1.87842	0.000552	0.128131
ENSG00000165125	<i>TRPV6</i>	7:142568956–142583507	0.559696	0.130914	2.081086	0.000573	0.130824